Fiber-Based Nonlocal Formulation for Simulating Softening in Reinforced Concrete Beam-Columns

Maha Kenawy, S.M.ASCE[1]; Sashi Kunnath, F.ASCE[2]; Subodh Kolwankar, S.M.ASCE[3]; and Amit Kanvinde, M.ASCE[4]

Abstract: A nonlocal formulation framework is presented to address mesh-dependent strain localization in displacement-based frame element models in the presence of constitutive softening. The framework consists of a nonlocal displacement-based frame element and a nonlocal fiber-based plasticity model, and is used to simulate the postpeak response of RC structural members. The algorithmic implementation of the framework is discussed, and its performance is thoroughly investigated. Mesh sensitivity studies reveal that the proposed approach eliminates mesh-dependent strain localization and leads to objective global (i.e., load displacement) and local (i.e., curvature profile) response in the presence of concrete softening. Comparison with historical test data from 24 column specimens shows that the postpeak response of RC beam-columns is predicted with reasonable accuracy. The limitations of the presented framework are discussed along with areas for further development. **DOI: 10.1061/(ASCE)ST.1943-541X.0002218.**

Author keywords: Nonlocal formulation; Frame elements; Localization; Concrete softening.

Introduction and Background

The simulation of extreme limit states in structures is an essential component of performance-based engineering. In RC beam-columns, these limit states are controlled by local instabilities at the material and cross-sectional levels, such as concrete crushing and rebar buckling on the compression side of the member and rebar necking and fracture on the tension side. These phenomena result in postpeak softening (negative stiffness) in the load-displacement response of the structural member, which indicates loss of member strength and eventually leads to structural collapse. Consequently, accurate and robust simulation of the softening response or strength degradation of beam-columns is a critical component of performance assessment of RC frame structures.

Current approaches to simulating nonlinear structural response (in research or practice) include continuum finite-element (FE) and line-element models. Continuum FE models are generally considered prohibitively expensive for large-scale simulations. As a result, line-element models are commonly used in structural simulations using one of two approaches: (1) concentrated or plastic hinge models, in which the nonlinear behavior is lumped into rotational springs at the member ends (Clough et al. 1965; Giberson 1967); or (2) distributed plasticity models, wherein the cross-sectional response at discrete locations along the member is integrated. In the latter type, the section behavior may be described by a stress-resultant plasticity model (El-Tawil and Deierlein 1998) or a fiber model, which aggregates uniaxial material response across each section. Distributed plasticity models, in turn, use one of two formulations: a displacement-based (DB) formulation, which follows the standard finite-element method; or a force-based (FB) formulation (Spacone et al. 1996a, b), which may be considered a frame-member interpretation of the mixed finite-element method (Zienkiewicz and Taylor 2005).

Although hinge-type models are computationally efficient, the locations of the plastic hinges in these models must be defined a priori, thereby preventing the simulation of damage initiation and propagation in a generic sense. Moreover, these models cannot conveniently capture the axial force–bending moment (P-M) interaction effects [an example of a plastic hinge model that incorporates P-M interaction was given by Powell and Chen (1986)]; as a result, they usually require component-based calibration based on the axial load level and moment gradient, and cannot be generalized across different components (Scott and Fenves 2006). These drawbacks are overcome in fiber-section models, which enable the formation of plastic hinges at any location and generic spread of plasticity along the member. However, the performance of fiber-based frame models is compromised when simulating the softening response of the member. In particular, two problems can be identified in the predictions of a fiber model simulation in the presence of constitutive softening: (1) nonobjectivity of the global response, i.e., the postpeak load-displacement response becomes highly sensitive to the member discretization (or the mesh size); and (2) localization of the strain field over a distance controlled by the member discretization, and the size of the localization zone approaches zero as the number of elements is increased.

In the context of continuum FE models, numerous studies have documented the mesh sensitivity of the load deformation response and strain localization associated with the modeling of softening materials (Bažant and Oh 1983; Bažant et al. 1987; Bažant and Jirásek 2002). Over the last several decades, various methods have been used to enhance the strain field and overcome these problems, most notably nonlocal continuum mechanics. The fundamental premise of the nonlocal continuum theory is that the response

[1]Graduate Research Assistant, Dept. of Civil and Environmental Engineering, Univ. of California, Davis, CA 95616 (corresponding author). ORCID: https://orcid.org/0000-0002-9722-091X. Email: mmkenawy@ucdavis.edu

[2]Professor, Dept. of Civil and Environmental Engineering, Univ. of California, Davis, CA 95616.

[3]Graduate Research Assistant, Dept. of Civil and Environmental Engineering, Univ. of California, Davis, CA 95616.

[4]Professor, Dept. of Civil and Environmental Engineering, Univ. of California, Davis, CA 95616.

Note. This manuscript was submitted on November 15, 2017; approved on June 5, 2018; published online on September 26, 2018. Discussion period open until February 26, 2019; separate discussions must be submitted for individual papers. This paper is part of the ***Journal of Structural Engineering***, © ASCE, ISSN 0733-9445.

(i.e., stress or force) at a material point depends on the deformation at the point and on the deformation profile in the vicinity of that point. The application of the nonlocal theory in continuum FE models was shown to prevent mesh-dependent strain localization in various constitutive frameworks; examples include nonlocal damage models (Pijaudier-Cabot and Bažant 1987; Bažant and Pijaudier-Cabot 1989), nonlocal smeared cracking models (Bažant and Lin 1988b; Jirásek and Zimmermann 1998), and nonlocal softening plasticity models (Bažant and Lin 1988a; Brinkgreve 1994).

The previous examples are of the so-called integral nonlocal formulations, which are the focus of this paper. In general, two main classes of nonlocal formulations exist, namely integral formulations and gradient formulations (explicit and implicit). Integral nonlocal models introduce weighted spatial averages of field quantities into the constitutive model. In the explicit gradient formulation, the integral is approximated with a truncated Taylor series for sufficiently smooth deformation fields. The nonlocal field is, therefore, given in terms of the local field and its second-order derivative, which introduces a spatial interaction for a continuous strain field. The presence of these higher-order derivative terms, however, imposes stronger continuity requirements on the displacement field than does the integral approach, which makes the explicit formulation computationally less attractive. This aspect is avoided in the implicit gradient formulation, which contains second-order derivatives of the nonlocal field instead, and was shown to be a special case of the integral nonlocal formulation (Peerlings et al. 2001). The implicit gradient and integral nonlocal formulations exhibit qualitatively equivalent behavior in different localization contexts (Peerlings et al. 2001). The implementation of the gradient formulation, however, requires solving the partial differential equation introduced into the model for the nonlocal variables. In contrast, the integral formulation requires only computing integral terms of existing variables. From the implementation point of view, the integral model may be considered more cumbersome because it requires data transfer between different elements. Nonetheless, it enforces the nonlocality in a more transparent way; the implications of this aspect are highlighted in the element formulation section of this paper.

In the context of frame-element models, Coleman and Spacone (2001) first noted the mesh sensitivity in FB element models of RC members, and several methods were subsequently proposed to address the problem (Scott and Fenves 2006; Addessi and Ciampi 2007; Valipour and Foster 2009; Feng et al. 2015; Sideris and Salehi 2016). Some of these methods were developed in the context of frame elements directly, whereas others were adapted from existing continuum FE approaches. Plastic hinge integration methods in FB elements are an example of the former type, wherein the integration along the element is manipulated to control localization via a priori specification of the location and length of the plastic hinge (Scott and Fenves 2006; Addessi and Ciampi 2007). The methods adapted from continuum FE may be categorized as either partial regularization techniques or true localization limiters. The crack band model (Bazant 1982; Bažant and Oh 1983) is a common partial regularization technique, originally used for simulating the tensile fracture in concrete continuum FE models and later extended to simulate the compressive softening of concrete in frame elements (Coleman and Spacone 2001; Pugh et al. 2015). The method is based on adjusting the material stress-strain relationship in coordination with the mesh size, to ensure constant energy dissipation across different levels of mesh refinement. This approach results in an objective load-displacement response; however, mesh-dependent localization of deformation is not mitigated.

On the other hand, nonlocal formulations are true localization limiters which imbed a material length scale into the model, and enforce a mesh-independent and physically-guided deformation field (e.g., inelastic strains or curvature profile). Addessi and Ciampi (2007) proposed an integral nonlocal formulation with a resultant section constitutive law for the flexural response, and adopted the formulation for both FB and DB elements. This formulation does not consider P-M interaction, and therefore requires calibration based on the axial load level. Valipour and Foster (2009) presented a fiber-based nonlocal FB frame element based on a secant stiffness approach and a damage model for concrete, with a characteristic length empirically expressed as a fraction of the beam length. The approach is based on a secant iteration scheme and is, consequently, less suited for implementation in tangent stiffness–based computer codes. Feng et al. (2015) and Sideris and Salehi (2016) developed fiber-based FB frame elements based on the implicit gradient approach, also using empirical plastic hinge lengths as the length-scale parameter. The key difference is that Sideris and Salehi (2016) incorporated the nonlocality in the strain-displacement equations, rather than the constitutive relations.

The preceding examples predominantly use FB element formulations. In the FB element, equilibrium is strictly satisfied, even with nonlinear material response. Although this feature provides the advantage of using very coarse meshes (typically one element per member), the solution algorithm typically involves the use of nested iterative loops. The nonlocal FB formulation presented by Sideris and Salehi (2016) overcomes this problem and yields a single system of algebraic equations to solve. However, the model has other limitations, including the need to enforce additional intermediate boundary conditions at localization locations and the inability of the model to accommodate multielement meshing (i.e., the entire beam-column member can only be modeled with a single element). The latter limitation means that the model, in its current form, cannot incorporate distributed loads along the member length.

For the DB element, very few studies have combined a DB formulation with a nonlocal approach, and virtually none in a fiber-based context. Zhang and Khandelwal (2016) presented a DB nonlocal model, also based on the implicit gradient approximation, with a section resultant constitutive relationship. The model uses an alternative framework, isogeometric analysis (Hughes et al. 2005), for constructing higher-order finite-element interpolation functions in order to approximate the higher-order gradient terms. Although theoretically attractive, the approach is relatively complicated to implement in existing finite-element codes.

A DB frame element formulation with nonlocal fiber-based constitutive relations is presented in this study. The proposed formulation combines the advantages of fiber-based models and the localization-limiting properties of the nonlocal theory. The formulation preserves the straightforward element state determination of the standard finite-element procedure and the ability to model members with distributed loads. The approach does not incorporate any additional boundary conditions or impose stronger continuity requirements on the interpolation functions. Additionally, the developed frame element is combined with an efficient method for approximating the nonlocal field variables that drive the softening response, proposed by Brinkgreve (1994), which improves the computational efficiency of the nonlocal averaging procedure. The proposed formulation and associated material model are implemented in the open source structural analysis platform OpenSees version 2.4.2 (McKenna 2000) and used to simulate the postpeak response of reinforced concrete beam-columns. The performance of the model is assessed via mesh sensitivity studies and validated against available experimental data.

The paper begins by articulating the motivation for nonlocal theories, and describing the nonlocal averaging procedure. The proposed element formulation is described in the consequent section and the novel nonlocal aspects are highlighted. Next, the

constitutive framework selected for the current study and the algorithmic implementation of the proposed formulation are discussed. This is followed by a summary of the numerical simulations conducted to assess the performance of the nonlocal model. The paper concludes with a discussion of the model limitations and areas for future work.

Nonlocal Theory: Concept and Physical Basis

Modeling of Concrete Damage in a Continuum

In frame and continuum simulations, progressive damage in heterogeneous brittle materials, such as concrete, is typically modeled at the constitutive level as strain-softening. Early experimental tests by several researchers (Van Mier 1984; Vonk 1993; Jansen and Shah 1997; Van Mier et al. 1997) confirmed that, under compressive loading, the damage within a concrete specimen tends to localize in a region of finite length. This localized damage is macroscopically measured over a certain gauge length and represented as softening (Fig. 1), whereas the rest of the specimen unloads elastically.

In a classical continuum with strain-softening, the boundary-value problem becomes ill-posed, which leads to the aforementioned mesh dependence of the solution (Bažant and Belytschko 1985; Bažant and Lin 1988a; Bažant and Jirásek 2002). This numerical phenomenon motivated the use of the nonlocal continuum, which is now widely recognized as an effective means of regularizing the strain-softening boundary-value problem. In the standard (local) FE continuum, the size of the localization zone depends artificially on the mesh size, and can become arbitrarily small upon mesh refinement. In the nonlocal continuum, on the other hand, a finite localization zone is obtained by considering interactions between neighboring material points within a prescribed interaction radius R. Theoretically, this interaction radius is determined by a material characteristic length, which is, in turn, informed by the heterogeneity of the microstructure—e.g., the maximum aggregate size in concrete (Bazant 1976; Bažant and Pijaudier-Cabot 1989). In a more practical sense, the interaction radius of the nonlocal continuum may be informed by the gauge length over which the localized damage is measured in an experimental setup. With this interpretation, the nonlocal theory serves to diffuse or distribute the damage over this gauge length to achieve consistency with experimental measurements. This concept is described mathematically in the following subsection.

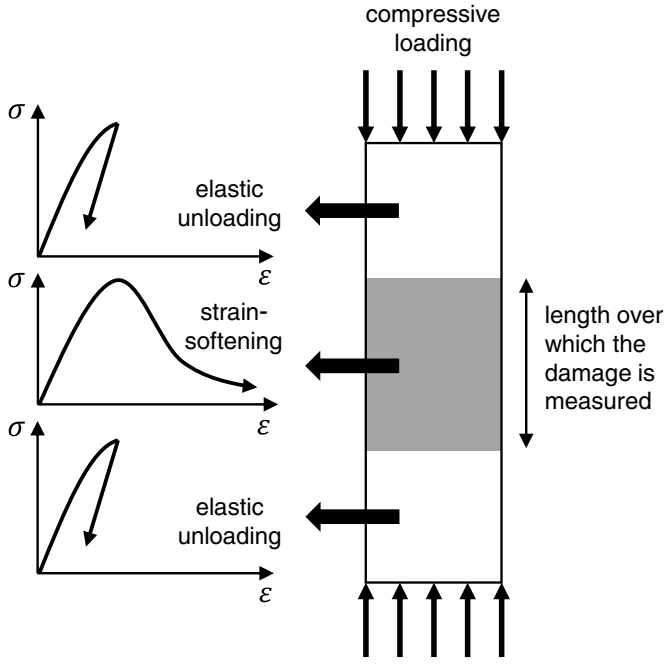

Fig. 1. Idealized damage localization in a concrete cylinder.

Nonlocal Averaging Concept

The formulation presented in this paper falls under the category of integral nonlocal models, wherein a local field variable is replaced by its nonlocal counterpart. The nonlocal variable $\widetilde{f(x)}$ at a location x is calculated as a weighted average of the local variable $f(x)$ over a spatial neighborhood of that location. In the one-dimensional context, this averaging procedure is expressed as

$$\widetilde{f(x)} = \int_L \bar{w}(x,r) f(r) dr \tag{1}$$

where L represents the entire one-dimensional domain; and $\bar{w}(x,r)$ = weighting function that satisfies the normalizing condition, such that the nonlocal averaging operator does not alter a uniform field, i.e.

$$\bar{w}(x,r) = \frac{w(x,r)}{\int_L w(x,r) dr} \tag{2}$$

The value of the weight function $w(x,r)$ depends solely on the distance between two spatial locations, determined by the difference between the global coordinate of the point x and the local coordinate of a neighboring point r. The choice of the weight function and the interaction radius of the nonlocal model determines the size of the localization zone and the strain distribution within the zone. A bell-shaped function is conventionally used as the weight function. In the proposed formulation, this function is defined as

$$w(r) = \left\langle 1 - \frac{r^2}{R^2} \right\rangle^2 \tag{3}$$

where R = interaction radius; and the Macaulay brackets $\langle \cdot \rangle$ indicate the positive part of the argument only. Fig. 2 plots this weight function; the horizontal axis represents the local coordinate r and the vertical axis represents the corresponding weight $w(r)$.

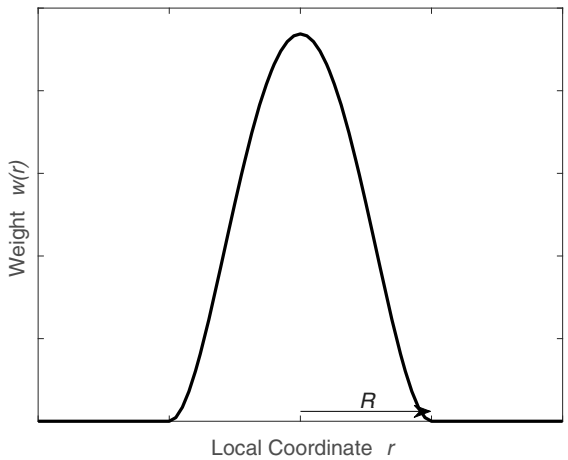

Fig. 2. Weight function used for nonlocal averaging.

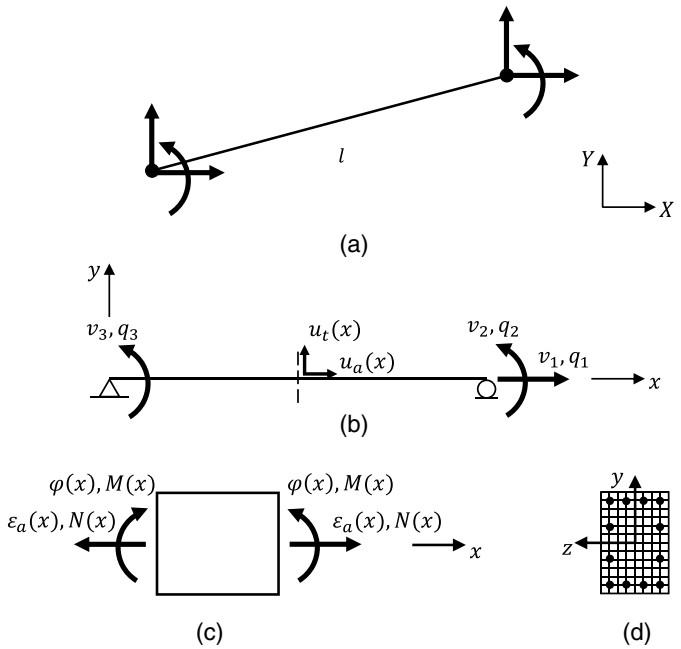

Fig. 3. Schematic representation of fiber-based frame element: (a) element global DOFs; (b) natural DOFs and corresponding element forces; (c) section deformations and corresponding forces; and (d) fiber-discretized cross section.

Nonlocal Displacement-Based Frame-Element Formulation

The nonlocal element formulation is derived by enriching the DB beam element with nonlocal section deformation variables. The nonlocal variables are obtained through a nonlocal averaging operation that incorporates interactions with neighboring sections over a certain interaction radius. The two-dimensional element formulation presented herein is based on Euler–Bernoulli beam theory. The main equations of the basic (local) formulation are presented first, and then the nonlocal enrichment of the formulation is illustrated. The element has six global degrees of freedom (DOFs) (Fig. 3). By transforming the DOFs to the local coordinate system and eliminating the rigid body modes, the element deformations vector $\mathbf{v}$ can be expressed as

$$\mathbf{v} = [\, v_1 \quad v_2 \quad v_3 \,]^T \tag{4}$$

and the corresponding vector of element forces $\mathbf{q}$ (Fig. 3) is

$$\mathbf{q} = [\, q_1 \quad q_2 \quad q_3 \,]^T \tag{5}$$

The interpolation of the displacement field can be expressed as

$$\mathbf{u}(x) = \mathbf{N}(x)\mathbf{v} \tag{6}$$

$$\mathbf{u}(x) = \begin{bmatrix} u_a(x) \\ u_t(x) \end{bmatrix} \tag{7}$$

where $\mathbf{u}(x)$ = vector of the axial and transverse displacements at each section along the element; and $\mathbf{N}(x)$ = matrix of the displacement shape functions, which uses the cubic Hermitian polynomials for transverse displacements and linear Lagrange polynomials for the axial displacement

$$\mathbf{N}(x) = \begin{bmatrix} \xi & 0 & 0 \\ 0 & \xi^3 - 2\xi^2 + \xi & \xi^3 - \xi^2 \end{bmatrix} \tag{8}$$

where $\xi = x/l$, where l = element length. This choice yields constant axial strain and linear curvature along the element length, and leads to the following kinematic relationship:

$$\mathbf{e}(x) = \mathbf{B}(x)\mathbf{v} \tag{9}$$

where $\mathbf{e}(x)$ = vector of section deformations

$$\mathbf{e}(x) = \begin{bmatrix} \varepsilon_a(x) \\ \varphi(x) \end{bmatrix} \tag{10}$$

where $\varepsilon_a(x) = u_a'(x)$ = section axial strain; $\varphi(x) = u_t''(x)$ = section curvature; and the strain-displacement matrix $\mathbf{B}(x)$ consists of shape function derivatives. The corresponding resultant section forces $\mathbf{s}(x)$ (Fig. 3) are

$$\mathbf{s}(x) = \begin{bmatrix} N(x) \\ M(x) \end{bmatrix} \tag{11}$$

which consist of the section axial force and bending moment. The changes in the section forces $\mathbf{s}(x)$ are related to changes in section deformations $\mathbf{e}(x)$ through the section stiffness matrix $\mathbf{k}_s$

$$\mathbf{k}_s = \frac{\partial \mathbf{s}}{\partial \mathbf{e}} = \begin{bmatrix} \dfrac{\partial N}{\partial \varepsilon_a} & \dfrac{\partial N}{\partial \varphi} \\ \dfrac{\partial M}{\partial \varepsilon_a} & \dfrac{\partial M}{\partial \varphi} \end{bmatrix} \tag{12}$$

Application of the principal of virtual displacement leads to the following equilibrium condition between the element forces $\mathbf{q}$ and the section forces $\mathbf{s}$:

$$\mathbf{q} = \int_0^l \mathbf{B}^T(x)\mathbf{s}(x)dx \approx \sum_{i=1}^{N_p} \mathbf{B}^T(x_i)\mathbf{s}(x_i)\Omega_i \tag{13}$$

Eq. (13) is evaluated using numerical quadrature over N_p number of sections along the element, where Gauss-Legendre is the selected as the integration rule. In the expression, Ω_i represents the quadrature weight associated with each integration point. In a similar fashion, the element stiffness matrix $\mathbf{K}$ is assembled from the individual section stiffness matrices as follows:

$$\mathbf{K} = \frac{\partial \mathbf{q}}{\partial \mathbf{v}} = \int_0^l \mathbf{B}^T(x)\mathbf{k}_s(x)\mathbf{B}(x)dx \approx \sum_{i=1}^{N_p} \mathbf{B}^T(x_i)\mathbf{k}_s(x_i)\mathbf{B}(x_i)\Omega_i \tag{14}$$

In the fiber-based formulation, each section is divided into a number of fibers N_f (Fig. 3), and the section forces are evaluated by aggregating the uniaxial stresses σ_j at each fiber location

$$\mathbf{s}(x_i) = \sum_{j=1}^{N_f} \mathbf{a}_j^T \sigma_j A_j \tag{15}$$

where A_j = cross-sectional area of fiber j; and $\mathbf{a}_j = [\, 1 \quad -y_j \,]$ = a transformation matrix, where y_j = location of fiber j in the cross section. Similarly, the fiber uniaxial strains are evaluated from the section deformations as

$$\varepsilon_j = \mathbf{a}_j \mathbf{e}(x_i) \tag{16}$$

The nonlocal formulation is obtained by introducing nonlocal deformation variables into the constitutive model. These nonlocal variables can be introduced as section deformations at the element

level, or as uniaxial strains at the section level. In the proposed formulation, the nonlocal section deformations $\tilde{\mathbf{e}}$ are evaluated as a weighted average of the corresponding local deformations at the neighboring sections

$$\tilde{\mathbf{e}}(x) = \int_L \bar{w}(r)\mathbf{e}(x,r)dr \tag{17}$$

where $\bar{w}(r)$ = normalized weight function presented in the preceding section; and L represents the entire domain. Because of the monotonically decreasing nature of the weight function, the contributions from neighboring sections die out as the distance r increases. Therefore, it is computationally efficient to use a weight function with a bounded support, such as the function in Eq. (3). Eq. (17) is also evaluated using numerical quadrature, leading to the following expression for the nonlocal deformation of section i, evaluated by averaging the deformations over N neighboring sections (determined by the interaction radius):

$$\tilde{\mathbf{e}}(x_i) = \frac{\sum_{k=1}^{N} w(r_k)\mathbf{e}(x_k)\Omega_k}{\sum_{k=1}^{N} w(r_k)\Omega_k} \tag{18}$$

where $w(r_k)$ and Ω_k = nonlocal weight and quadrature weight, respectively, associated with section k; and r_k = distance between sections i and k. The expression represents a normalized weighted average which does not alter a uniform field, as explained in the preceding section. The nonlocal uniaxial fiber strains $\tilde{\varepsilon}$ are evaluated in a manner similar to Eq. (16)

$$\tilde{\varepsilon}_j = \mathbf{a}_j\tilde{\mathbf{e}}(x_i) \tag{19}$$

Finally, the fiber stresses and strains are related through a constitutive relationship, in which the uniaxial stresses depend on both the local and nonlocal uniaxial strains. The constitutive model used in this work is described in the following section.

The assumption that plane sections remain plane, which follows from Euler–Bernoulli beam theory, implies no interaction between the individual fibers in a cross section. This limitation means that shear deformations are not considered in the element formulation. Extension of the nonlocal formulation to shear-deformable beams—for example, the mixed formulation beam element by Filippou and Saritas (2006)—warrants further investigation.

Furthermore, in the context of the nonlocal formulation, the forces at a section i are now a function of the deformations at section i, and the deformations at the neighboring sections. This can be expressed as

$$\mathbf{s}(x_i) = \mathbf{s}(\mathbf{e}(x_i), \tilde{\mathbf{e}}(x_i, \mathbf{e}(x_k))) \tag{20}$$

where subscript k implies summation over N neighboring sections. The stiffness matrix for section i can be evaluated by taking the derivative of the section forces vector in Eq. (20), with respect to both of its arguments

$$\mathbf{k}_s^{nl}(x_i) = \frac{\partial \mathbf{s}(x_i)}{\partial \mathbf{e}(x_k)} = \frac{\partial \mathbf{s}(x_i)}{\partial \mathbf{e}(x_i)}\delta_{ik} + \frac{\partial \mathbf{s}(x_i)}{\partial \tilde{\mathbf{e}}(x_i)}\frac{\partial \tilde{\mathbf{e}}(x_i)}{\partial \mathbf{e}(x_k)} \tag{21}$$

where δ_{ik} = Kronecker delta, and no summation is implied over the subscript i; the first term on the right-hand side of the equation represents the local section stiffness; and the second term is obtained using the chain rule. Substituting into Eq. (14) for the element stiffness matrix gives

$$\mathbf{K} = \sum_{i=1}^{N_p} \mathbf{B}^T(x_i)\mathbf{k}_s(x_i)\mathbf{B}(x_i)\Omega_i + \sum_{i=1}^{N_p}\sum_{k=1}^{N} \mathbf{B}^T(x_i)\widetilde{\mathbf{k}_s}(x_i)\frac{\partial \tilde{\mathbf{e}}(x_i)}{\partial \mathbf{e}(x_k)}\mathbf{B}(x_k)\Omega_i \tag{22}$$

where $\widetilde{\mathbf{k}_s}(x_i) = \partial \mathbf{s}(x_i)/\partial \tilde{\mathbf{e}}(x_i)$; N_p = number of integration points along the element; and N = number of integration points (or sections) included in the nonlocal averaging operation, and typically spans several elements. The second term on the right-hand side represents an additional nonlocal contribution to the element stiffness matrix. The current numerical implementation of this formulation ignores the nonlocal term, and approximates the element stiffness matrix by the local stiffness matrix (the first term only). Although using the fully consistent tangent stiffness matrix typically accelerates convergence, it may be argued that the nonlocal term in Eq. (22) increases the bandwidth of the stiffness matrix and, correspondingly, increases the computational expense. This issue may require further investigation to weigh this expense against that required for convergence with an approximate local stiffness matrix. Such investigation is, however, outside the scope of this paper.

Eqs. (18) and (19), in combination with the constitutive model presented in the following section, represent the nonlocal enrichment of the conventional DB element formulation. The following observations can be made:

1. Eq. (18) requires communication of the deformation data between neighboring sections within a given element, as well as sections in the neighboring elements. The extent of the interaction with neighboring sections depends on the selected length scale or interaction radius associated the weighting function in Eq. (3).
2. The nonlocality in the current formulation is introduced through integral terms of existing quantities of the deformation field (section deformations or fiber strains). The formulation does not incorporate additional intermediate boundary conditions or impose stronger continuity requirements on the interpolation functions of the finite element solution.
3. The proposed model enforces the nonlocality at the constitutive level, through appropriately enriched material models. This aspect has the following implications:
   - The formulation imposes constraints on the form of the constitutive model used in combination with the proposed nonlocal DB element (the stress is a function of the local and nonlocal strains).
   - The imposed length scale (through the interaction radius of the weight function) may be attributed a physical meaning that is directly related to strain measurements in a uniaxial experiment. The interpretation of this length-scale parameter in the current study was briefly discussed in the preceding section, and is quantatively specified subsequently.
   - The formulation may be directly extended to model multiple softening responses with different length parameters within the same section; a feature that may be suited for modeling multiple localization phenomena in composite sections (for example, concrete crushing and rebar buckling in a RC section). Such phenomena may be difficult to accommodate using recent gradient frame-element formulations which enforce the nonlocality in the strain-displacement relationship of the element (e.g., Sideris and Salehi 2016) using a single, and somewhat empirical, length-scale parameter.

Nonlocal Constitutive Model

A bilinear softening plasticity model is used to model the concrete response in the proposed framework. The basic (local) form of the model is presented first, and then the nonlocal enrichment is described. The model retains the typical one-dimensional equations of elastoplasticity, which consist of a yield function that has the form

$$f(\sigma,\kappa) = \|\sigma\| - \sigma_y(\kappa) \tag{23}$$

where σ = stress; and κ = hardening/softening variable. The evolution of the yield stress is described by a hardening/softening law. A linear softening law has the form

$$\sigma_y(\kappa) = \sigma_o + H\kappa \tag{24}$$

where H = plastic modulus, such that $H < 0$ for softening materials. The model also includes the following stress-strain relationship, flow rule, and consistency conditions, respectively

$$\sigma = E(\varepsilon - \varepsilon^p) \tag{25}$$

$$\dot{\varepsilon}^p = \dot{\lambda}\text{sign}(\sigma) \tag{26}$$

$$\dot{\lambda} \geq 0, \quad f(\sigma,\kappa) \leq 0, \quad \dot{\lambda} f(\sigma,\kappa) = 0 \tag{27}$$

where E = elastic modulus; ε and ε^p = total and plastic strain, respectively; and $\dot{\lambda}$ = rate of the plastic multiplier. Finally, the rate of the hardening/softening variable is related to the plastic strain rate by

$$\dot{\kappa} = \|\dot{\varepsilon}^p\| \tag{28}$$

The simplest nonlocal plasticity formulation is obtained by replacing the local softening variable κ with its nonlocal counterpart $\tilde{\kappa}$, defined as

$$\tilde{\kappa} = \int_L \bar{w}(x,r)\kappa(r)dr \tag{29}$$

This so-called purely nonlocal form leads to regularizing the global response (i.e., the load-displacement), but it does not prevent mesh-dependent strain localization. The same result was noted by Planas et al. (1993), Brinkgreve (1994), and Bažant and Jirásek (2002). This problem is resolved by the overly nonlocal model in which the local softening variable κ is replaced by a linear combination of the local and nonlocal counterparts. This combination is herein referred to as $\bar{\kappa}$, and is defined as

$$\bar{\kappa} = m\int_L \bar{w}(x,r)\kappa(r)dr + (1-m)\kappa \tag{30}$$

Accordingly, the consistency conditions in Eq. (27) now become

$$\dot{\lambda} \geq 0, \quad f(\sigma,\bar{\kappa}) \leq 0, \quad \dot{\lambda} f(\sigma,\bar{\kappa}) = 0 \tag{31}$$

and the rest of the equations remain the same. This formulation was first proposed by Brinkgreve (1994), and has been adopted in different constitutive frameworks (e.g., Strömberg and Ristinmaa 1996; Bažant and Di Luzio 2004; Grassl and Jirásek 2006). Eq. (30) introduces a weighting parameter m which must take values greater than 1.0, thereby attributing a higher weight to the nonlocal model (hence the name overly nonlocal). Using $m > 1.0$, therefore, ensures that zones of low local plastic strain get higher nonlocal plastic strain, which leads to effective distribution of the plastic strains over the localization zone (Brinkgreve 1994). The local and the simple nonlocal formulations are recovered when $m = 0.0$ and 1.0, respectively. In addition to the interaction radius R, m is a model parameter that likewise affects the size of the localization zone and, correspondingly, the slope of the softening response.

In a monotonic loading context, the value of the softening variable represents the equivalent plastic strain, i.e., $\kappa = \|\varepsilon^p\|$; therefore $\bar{\kappa}$ can be expressed as

$$\bar{\kappa} = (1-m)\|\varepsilon^p(x)\| + m\int_L \bar{w}(r)\|\varepsilon^p(x+r)\|dr \tag{32}$$

In the local material model, the consistency conditions [Eq. (27)] for all Gauss points are uncoupled, i.e., they can be solved for each Gauss point separately for the increment of the plastic multiplier. In contrast, in the nonlocal model, the value of the yield stress at each Gauss point depends on the value of the softening variable (and therefore the plastic multiplier) at the neighboring Gauss points. Consequently, the consistency conditions become coupled, and a system of equations for all Gauss points within the softening zone needs to be solved; Rolshoven (2003) presented a detailed implementation of the stress return algorithm for nonlocal softening models. The computational expense associated with the aforementioned approach can be circumvented by making suitable approximations of the nonlocal plastic strain. Recognizing that the plastic response usually dominates the elastic response, the averaging terms of the plastic strains in Eq. (32) can be approximated by the total strains (which are directly calculated from the loading and boundary conditions of the problem). Using this approach, the consistency conditions for all Gauss points remain uncoupled, and the need to solve a system of equations for multiple points is eliminated. This approximation was first introduced by Brinkgreve (1994). The nonlocal softening variable can now be expressed as

$$\bar{\kappa} = \|\varepsilon^p(x)\| - m\|\varepsilon\| + m\|\tilde{\varepsilon}\| \tag{33}$$

where

$$\tilde{\varepsilon} = \int_L \bar{w}(r)\varepsilon(x+r)dr \tag{34}$$

The approximation in Eq. (33) indicates that the nonlocal softening variable at a material point (i.e., a fiber location in the cross section) can now be evaluated using the local quantities at the point (the softening variable and total strain) in addition to the nonlocal total strain at the point; the latter is evaluated using the proposed nonlocal element formulation.

The proposed nonlocal element formulation, in combination with the nonlocal constitutive model described herein, was implemented in OpenSees and its perfomance was investigated, as discussed in the following section. The algorithmic implementation scheme is illustrated in Fig. 4, which omits the constitutive equations for brevity. A detailed description of the stress-return algorithm was given by Brinkgreve (1994).

Assessment of Proposed Nonlocal Framework

The performance of the proposed framework was assessed via a series of numerical simulations which compared the nonlocal model predictions with those of the conventional (local) model and with experimental data. The test problem was a RC cantilever column subjected to constant axial load, and monotonically increasing lateral displacements (Fig. 5). The following parameters defined the problem: (1) the axial load ratio, which is defined as $\eta = P/(f_c A_g)$, where P is the axial load, f_c is the unconfined concrete strength, and A_g is the gross concrete area in the section; (2) the volumetric transverse reinforcement ratio ρ_t, which characterizes the confinement of the concrete in the column; and (3) the shear span:depth ratio, defined as M/Vd, where M/V is the moment:shear ratio (for a cantilever beam loaded at the tip with a lateral force, this ratio is the beam length L) and d is the section depth. The response quantities of interest were the lateral

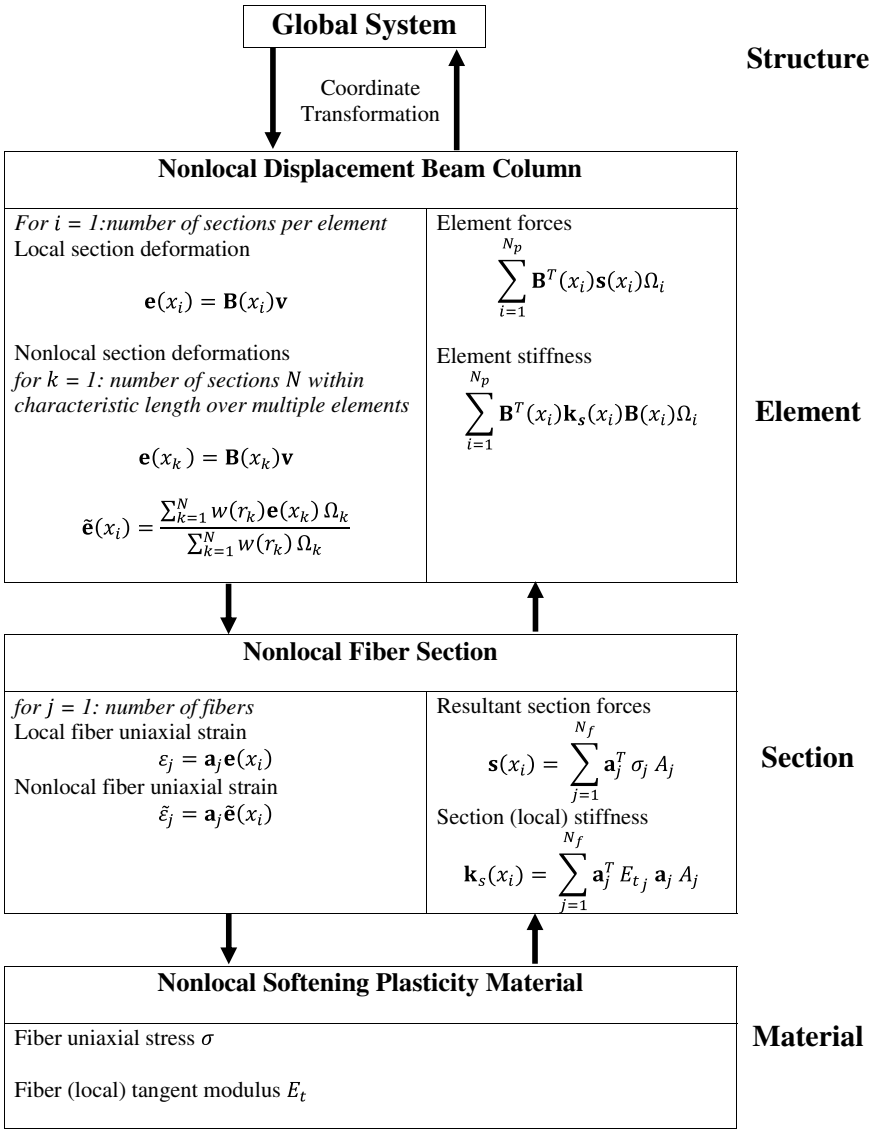

Fig. 4. Algorithmic implementation of nonlocal element formulation in OpenSees.

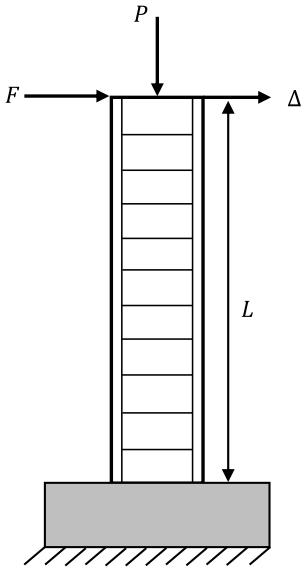

Fig. 5. Configuration of test problem.

load-displacement response (global response), and the curvature profile along the column (local response). The objective of the numerical investigation was to examine the ability of the proposed approach to robustly and accurately simulate the global and local response of the column. To this end, the numerical study consisted of the following two phases:

1. A mesh sensitivity study, in which the sensitivity of the simulation results to the choice of the member discretization (or mesh size) was examined over a practical range of problem parameters. The results obtained using the proposed nonlocal approach were compared with those obtained with the conventional analysis methodology.
2. Comparison with experimental data, in which the predicted response of 24 RC columns was validated against the observed response in laboratory experiments.

To appropriately compare the simulation results to experimental data in Phase 2, the material parameters were carefully selected to represent the constitutive response observed in the experiments. The selection of these parameters, in addition to the nonlocal model parameters, is discussed in the following subsection, followed by a summary of each phase of the numerical investigation.

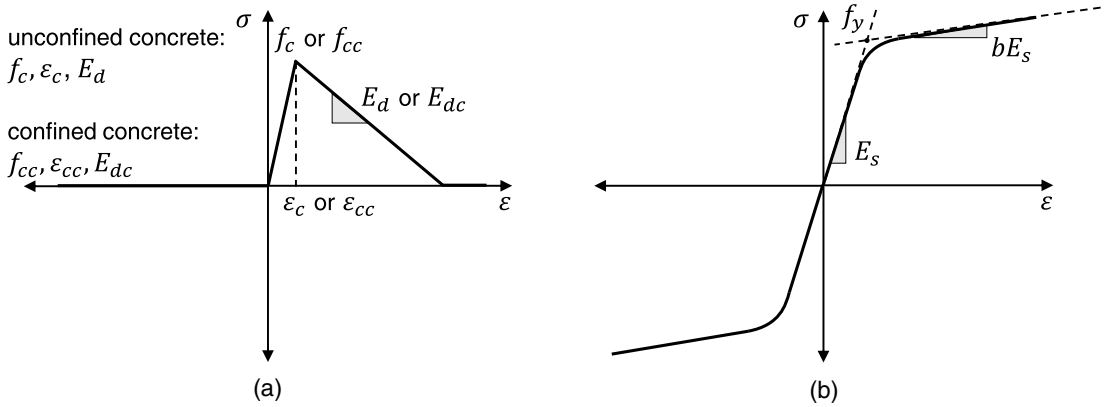

Fig. 6. Material models adopted in simulations: (a) unconfined and confined concrete; and (b) longitudinal steel reinforcement.

Selection of Material Parameters

In the simulation models, the cross section of the column consisted of fibers of unconfined and confined concrete, and layers of longitudinal reinforcing steel [Fig. 3(d)]. Fig. 6 shows a schematic representation of the response of each material. The nonlocal bilinear softening material was used to model the response of the concrete. Both the unconfined and confined concrete had no tensile strength; the compressive response is shown on the positive side for the concrete [Fig. 6(a)]. The Steel02 material in OpenSees [Giuffré-Menegotto-Pinto model by Menegotto and Pinto (1973)] was used to model the response of the reinforcing bars with a symmetric behavior in tension and compression [Fig. 6(b)]. Fracture of the rebar in tension and buckling in compression was not considered in the simulation models, because the primary purpose of the study was to simulate concrete damage in compression. These mechanisms, however, have a significant effect on the response of RC columns at ultimate limit states and are the subject of ongoing studies by the authors. The strength of the unconfined concrete f_c and the yield stress of the reinforcing bars f_y (Fig. 6) were obtained from the experimental data directly. For the remaining material parameters, the following assumptions were made:

Steel Reinforcement

The elastic modulus E_s of the steel was assumed to be 200 GPa, and the strain-hardening ratio b (the ratio of the postyield tangent to the initial elastic tangent modulus) was assumed to be 1% unless reported otherwise. In cases where the experimental stress-strain curve of the reinforcement was provided, a bilinear approximation of the curve was used in the simulation model. For the elastic-plastic transition parameters of Steel02 material, OpenSees recommended values were adopted ($R0 = 15$, $cR1 = 0.925$, and $cR2 = 0.15$). These parameters control the radius of curvature of the transition between the initial elastic branch and the postyield branch of the steel material.

Unconfined Concrete

The concrete strain at maximum stress ε_c was assumed be 0.002, which is a generally accepted value in the literature. Because the adopted material model is bilinear (i.e., the behavior was approximated as elastic until the onset of softening), the elastic modulus E_c is directly calculated as f_c/ε_c. The deterioration rate or softening slope (referred to in the figure as E_d) was determined such that the spalling strain (strain at zero stress) was 0.008. This was an approximate value based on observations from experimental tests on normal-weight concrete, which indicated that the spalling strain of the unconfined concrete was in the range 0.006–0.010. However, the choice of the spalling strain of the unconfined concrete had little or no influence on the response of the beam-column specimens in the validation study, and the overall behavior of the RC section was controlled primarily by the confined concrete.

Confined Concrete

The properties of the confined concrete, particularly the maximum stress f_{cc} and the deterioration rate or softening slope E_{dc}, strongly control the overall postpeak response of the column. Consequently, accurate estimation of these parameters guarantees consistency of the comparison of the simulated and experimentally observed responses, and is a key ingredient in the model validation process. Therefore, a separate study was conducted to select an appropriate confinement model. The details of the study, which compared four commonly used confinement models, are reported in the Appendix. The modified Kent and Park model (Scott et al. 1982) was selected for the current study because it balanced accuracy with simplicity. Scott et al. (1982) provide an overview of the equations used to predict the maximum concrete stress f_{cc}, concrete strain at maximum stress ε_{cc}, and the softening slope E_{dc}.

Nonlocal Length-Scale Parameter

The nonlocal interaction radius R affects the length of the plastic curvature zone in the column, the value of the maximum curvature, and the overall postpeak response of the member. In reference to the preceding discussion of compressive damage in concrete, this

Table 1. Parameters of test problems created for mesh sensitivity study

Number	Shear span:depth ratio, L/d	Axial load ratio, $\eta = P/(f_c A_g)$	Transverse reinforcement ratio, ρ_t
1	4.70	0.35	0.020
2	4.70	0.10	0.020
3	4.70	0.65	0.020
4	4.70	0.35	0.010
5	4.70	0.35	0.040
6	2.58	0.35	0.015
7	2.58	0.10	0.015
8	2.58	0.65	0.015
9	2.58	0.35	0.008
10	2.58	0.35	0.031

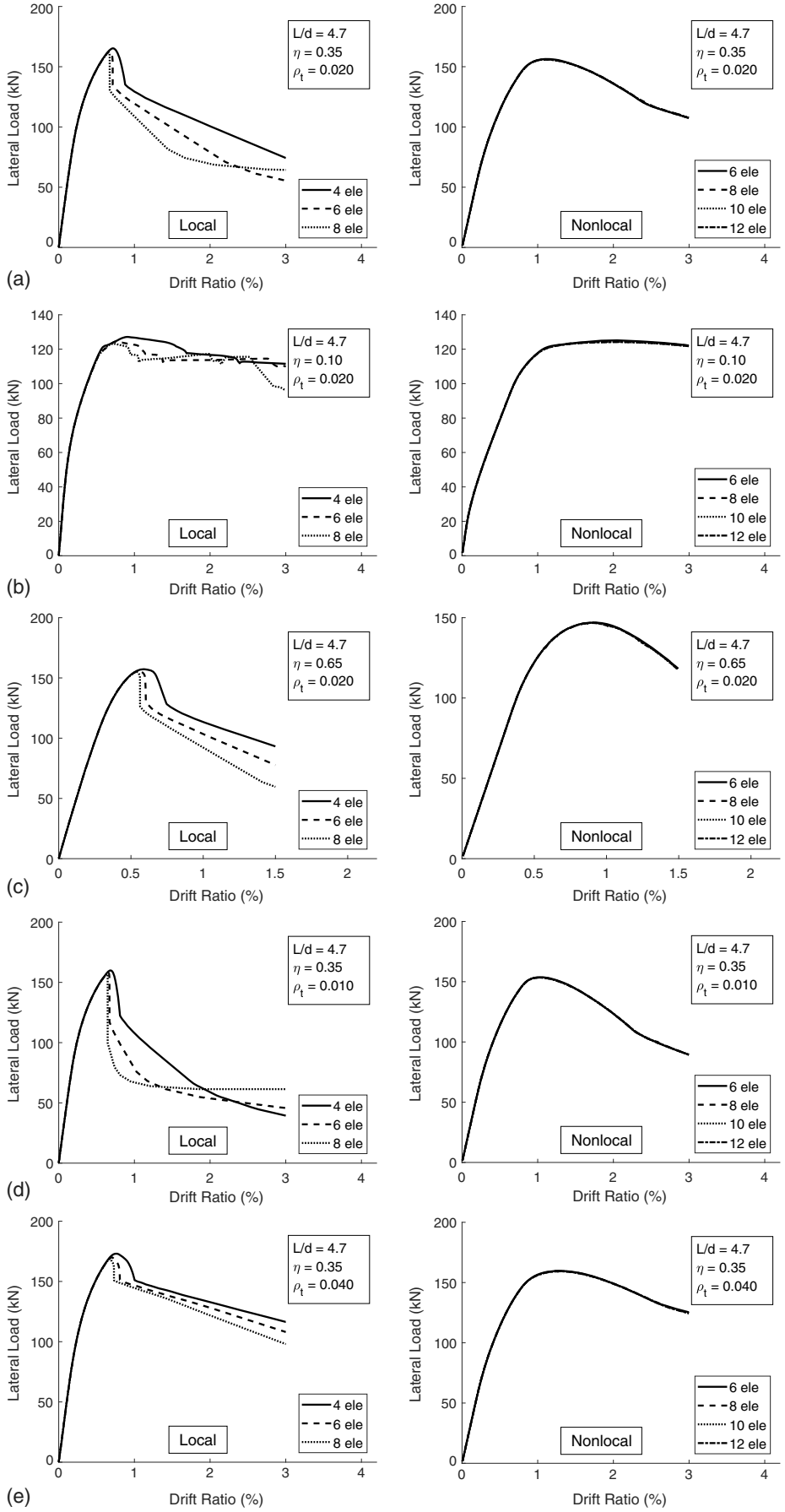

Fig. 7. Load-displacement response predicted using nonlocal and local models: (a) Test Problem 1; (b) Test Problem 2; (c) Test Problem 3; (d) Test Problem 4; and (e) Test Problem 5.

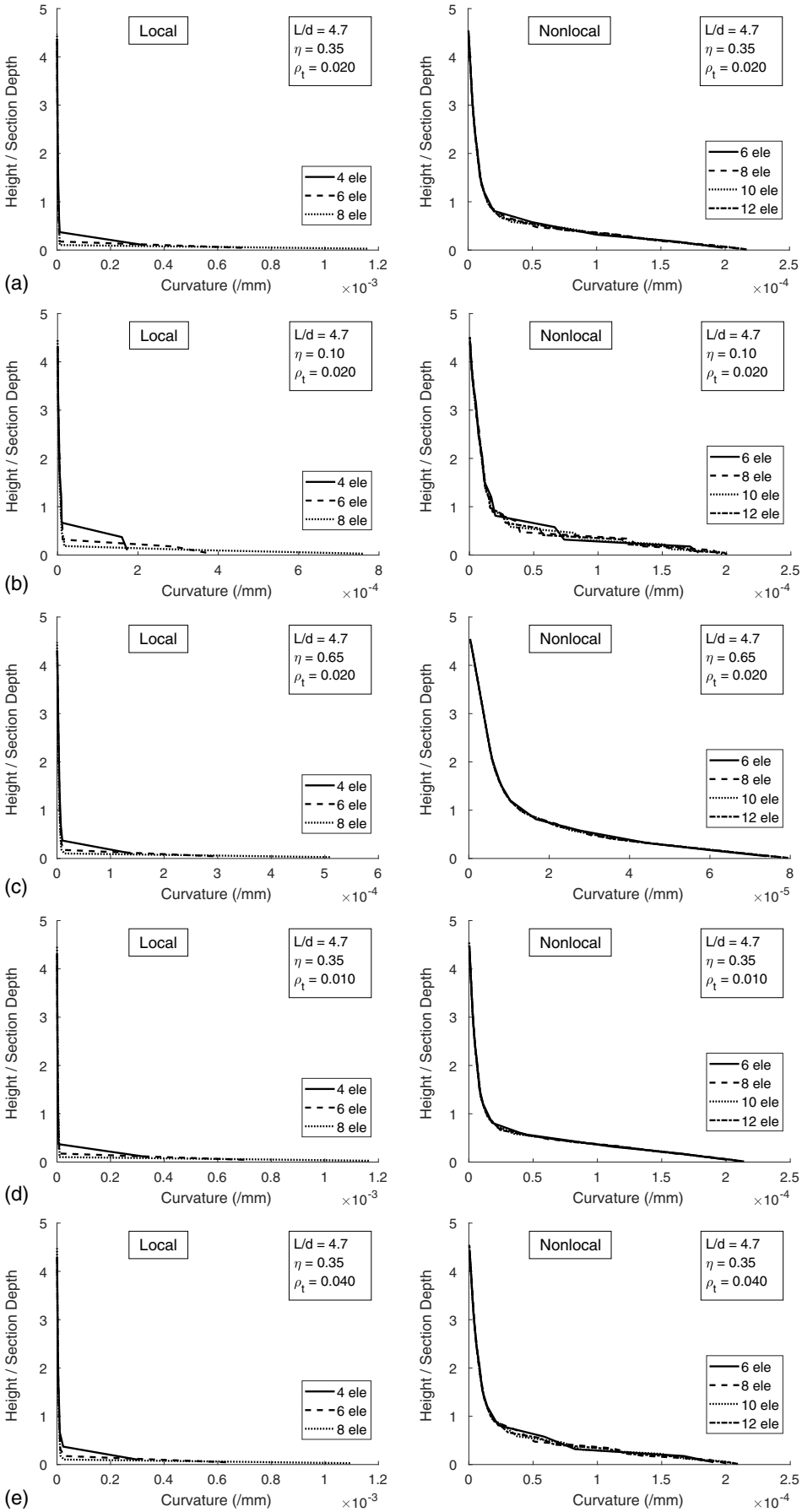

Fig. 8. Curvature profile predicted using nonlocal and local models: (a) Test Problem 1; (b) Test Problem 2; (c) Test Problem 3; (d) Test Problem 4; and (e) Test Problem 5.

parameter can be interpreted to effectively represent the gauge length associated with a strain-softening relationship (and, therefore, a certain softening slope), i.e., the length over which the strain is measured in an experimental setup. In the specific case of confined concrete, the softening slope of the confined concrete is typically predicted via a confinement model that consists of regressed equations based on small or full scale RC column tests. Consequently, the softening slopes dictated by these models have clearly defined length scales. The interaction radius can, therefore, be directly inferred from the confinement model. This study adopted the length scale associated with the modified Kent and Park confinement model. This value was reported by Scott et al. (1982) as 400 mm, and was used for all numerical examples. For general application of the proposed approach, the appropriate length scale associated with the confinement model or experimental stress-strain curve should be used. It should be noted that the size of the specimens in the Kent and Park experiments was 1,200 × 450 × 450 mm, and therefore size effects may be present if this confinement model is used to predict the properties of confined concrete in larger columns. However, this is an inherent artifact of the confinement model, and is not addressed in the proposed approach. In addition, the present research studied only cantilever columns in which the localization initiated at the domain boundary. In this particular case, the interaction radius was conveniently interpreted to be equivalent to the characteristic length. In circumstances where localization occurs farther from the boundary, the interaction radius is half of the characteristic length. Jirásek and Rolshoven (2003) further discussed the difference between localization zones close to and far from the domain boundary.

Nonlocal Weighting Parameter

The weighting parameter m was selected somewhat arbitrarily to be 1.5. As previously discussed, m must take values larger than 1.0 to mitigate mesh-dependent strain localization (Brinkgreve 1994). Choosing m in the range 1.2–2.0 had minimal effect on the response.

Mesh Sensitivity Study

Table 1 lists the parameters of the test problems created for this study, which included three different levels of axial load ratios and transverse reinforcement ratios for two columns with shear span: depth ratios of 2.58 and 4.70. For each test problem, a pair of simulation models was created as follows: (1) a simulation model which used the proposed nonlocal framework (herein referred to as the nonlocal model); and (2) a simulation model which used the conventional approach and Concrete02 material in OpenSees (referred to as the local model). Both simulation models used successively refined meshes (i.e., different number of elements per member), and two variations of the mesh density, either a uniform or a nonuniform mesh; in the latter, the element size varied along the member to provide a higher resolution of the plastic hinge region. The Gauss-Legendre quadrature rule was used, with two Gauss points per element. The results of each simulation pair (the load-displacement response and the curvature profile along the column) were compared.

Fig. 7 shows the lateral load versus drift ratio predicted by both approaches for Test Problems 1–5, and Fig. 8 shows the predicted curvature profile for the same test problems at the last step of the analysis (at 3% drift ratio for Problems 1, 2, 4, and 5, and 1.5% drift ratio for Test Problem 3). The following observations can be made from the figures:

- Although both approaches predicted the peak capacity of the column objectively, the postpeak response predicted by the local model exhibited severe mesh sensitivity. As the mesh was refined, the postpeak slope became steeper, resulting in severe convergence problems in the local model. This was particularly noticeable in test problems with high axial load ratios (represented by Test Problem 3 in Fig. 7). This was not unexpected, because in such cases most of the column section is in compression, and the postpeak response is primarily controlled by the concrete softening.
- On the other hand, the load-displacement response predicted by the nonlocal model was unaffected by the mesh size.

Table 2. Properties of column specimens tested in laboratory

Number	Reference	Length, L (mm)	Section depth, d (mm)	Axial load ratio, $\eta = P/(f_c A_g)$	Unconfined concrete strength, f_c (MPa)	Transverse reinforcement ratio, ρ_t	Longitudinal reinforcement ratio, ρ_l
1	Ang et al. (1981), Specimen 3	1,600	400	0.38	23.6	0.028	0.015
2	Ang et al. (1981), Specimen 4	1,600	400	0.21	25.0	0.022	0.015
3	Atalay and Penzien (1975), Specimen 11	1,676	305	0.28	31.0	0.015	0.016
4	Atalay and Penzien (1975), Specimen 10	1,676	305	0.27	32.4	0.009	0.016
5	Atalay and Penzien (1975), Specimen 6S1	1,676	305	0.18	31.8	0.009	0.016
6	Gill et al. (1979), Specimen 1	1,200	550	0.26	23.1	0.015	0.018
7	Gill et al. (1979), Specimen 3	1,200	550	0.42	21.4	0.018	0.018
8	Kanda et al. (1988), 85STC-1	750	250	0.11	27.9	0.011	0.016
9	Kono and Watanabe (2000), D1N60	625	242	0.66	37.6	0.015	0.024
10	Kono and Watanabe (2000), D1N30	625	242	0.33	37.6	0.015	0.024
11	Saatcioglu and Grira (1999), BG-1	1,645	350	0.43	34.0	0.010	0.020
12	Saatcioglu and Grira (1999), BG-2	1,645	350	0.43	34.0	0.020	0.020
13	Saatcioglu and Grira (1999), BG-3	1,645	350	0.20	34.0	0.020	0.020
14	Saatcioglu and Grira (1999), BG-4	1,645	350	0.46	34.0	0.013	0.029
15	Saatcioglu and Grira (1999), BG-8	1,645	350	0.23	34.0	0.013	0.029
16	Soesianawati et al. (1986), Specimen 1	1,600	400	0.10	46.5	0.009	0.015
17	Soesianawati et al. (1986), Specimen 2	1,600	400	0.30	44.0	0.012	0.015
18	Soesianawati et al. (1986), Specimen 3	1,600	400	0.30	44.0	0.008	0.015
19	Soesianawati et al. (1986), Specimen 4	1,600	400	0.30	40.0	0.006	0.015
20	Tanaka and Park (1990), Specimen 1	1,600	400	0.20	25.6	0.026	0.016
21	Tanaka and Park (1990), Specimen 7	1,650	550	0.30	32.1	0.021	0.013
22	Watson and Park (1989), Specimen 5	1,600	400	0.50	41.0	0.014	0.015
23	Watson and Park (1989), Specimen 9	1,600	400	0.70	40.0	0.048	0.015
24	Zahn et al. (1985), Specimen 7	1,600	400	0.22	28.3	0.016	0.015

The mesh-objectivity of the results was evident across the entire range of simulations. Additionally, whereas the formulation added a layer of computational effort to the analysis, the nonlocal model simulations exhibited superior convergence behavior compared with the local model.

- The curvature profile predicted by the local model (left-hand side of Fig. 8) suffered from localization of the plastic curvature into a single element at the base of the column for all cases, leading to mesh-dependent values of the maximum curvature and the length of the plastic hinge. In contrast, the nonlocal model (right-hand side of Fig. 8) successfully predicted a unique curvature profile and eliminated the mesh dependence of the curvature values and distribution.
- The mesh convergence of the nonlocal simulations characterized by a low axial-load ratio (e.g., Test Problem 2 in Fig. 8) was relatively slow compared with the remaining set, meaning that finer meshes were needed to obtain a converged curvature distribution. This phenomenon may be attributed to the fact that most of the concrete section was in tension, which possessed zero load-carrying capacity in the current model. In such problems, the nonlocal effect becomes less pronounced as the response is no longer controlled by compressive softening. In contrast, in test problems with relatively high axial load ratios (Test Problems 1, 3, 4, and 5 in Fig. 8), the curvature profile rapidly converged using a relatively coarse mesh size.

The effect of the mesh density variation on the convergence of the curvature profile is perhaps relevant to the present discussion; using a nonuniform mesh accelerates the mesh convergence in the nonlocal model because it permits a higher resolution of the plastic curvature at the hinge zone compared with a uniform mesh with the same number of elements (used for Test Problems 6 through 10—not depicted in the figures). This contrasts with the local model, in which the mesh sensitivity is accentuated with the nonuniform mesh, because the size of the first element (in which the curvature localizes) is much smaller than its counterpart in the uniform mesh.

Furthermore, in order for the nonlocal formulation to be effective, the member discretization needs to be such that the length (or integration weight) associated with a single Gauss point is smaller than the interaction radius of the nonlocal model (therefore allowing interaction with at least one neighboring Gauss point).

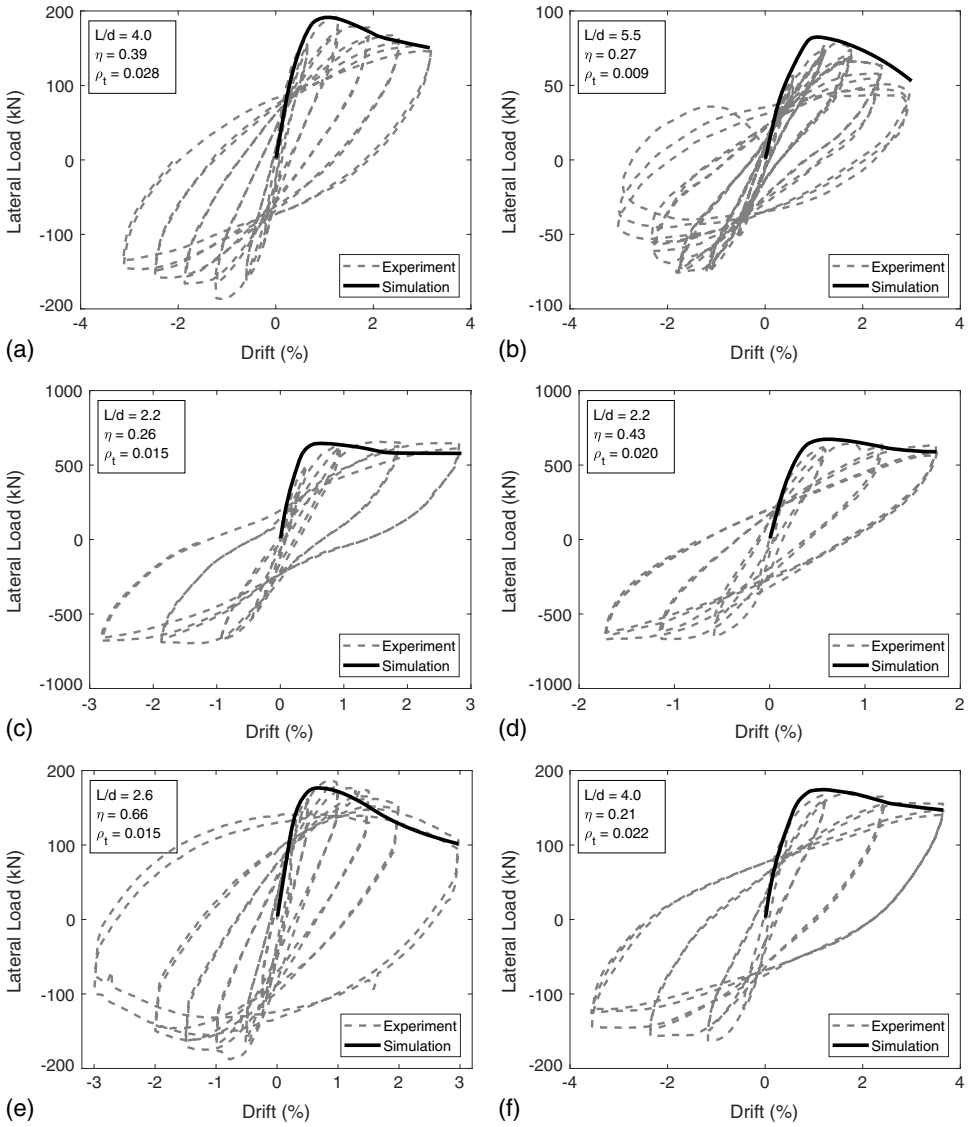

Fig. 9. Predicted and experimentally observed load-displacement response: (a) Ang et al. (1981), Specimen 3; (b) Atalay and Penzien (1975), Specimen 10; (c) Gill et al. (1979), Specimen 1; (d) Gill et al. (1979), Specimen 3; (e) Kono and Watanabe (2000), D1N60; and (f) Ang et al. (1981), Specimen 4.

For the columns used in this study, this constraint was achieved with as few as three or four elements per member and two Gauss points per element. However, this is a constraint for the nonlocality of the model to take effect, and does not eliminate the general need for sufficient discretization in DB elements to accurately interpolate nonlinear deformation fields. In the mesh sensitivity study conducted herein, a discretization of 6–10 elements per member seemed to achieve satisfactory nonlinear curvature profile for all test problems.

Comparison with Experimental Results

For this phase of the study, a database of 24 laboratory experiments, obtained from the PEER Structural Performance Database (Berry et al. 2004), was assembled to provide benchmark response data across a wide range of section dimensions, transverse confinement ratios, tie configurations, and axial load ratios. The properties of the columns tested in the experiments are summarized in Table 2; all columns had square sections with depth d ranging between 242 and 550 mm, and shear span:depth ratios M/Vd between 2.18 and 5.5. The ratio of the axial load on the column ranged between 0.1 and 0.7 of the nominal axial capacity, and all the specimens were reported to fail in flexure. Each column was subjected to monotonic lateral displacements, and the predicted force-deformation backbone was compared with the available cyclic data of each experiment. Additionally, the predicted curvature profile was compared with the experimentally observed curvature values at discrete locations along the column, if such measurements were available.

Figs. 9 and 10 show the predicted response of 12 columns overlaid on the corresponding experimental data for each column. These results are representative of the simulations conducted for all the specimens in Table 2. To establish the context of the comparison between the predicted and the experimentally observed response, it is noted that the nonlocal material model does not capture cyclic degradation. Therefore, its efficacy may be appropriately

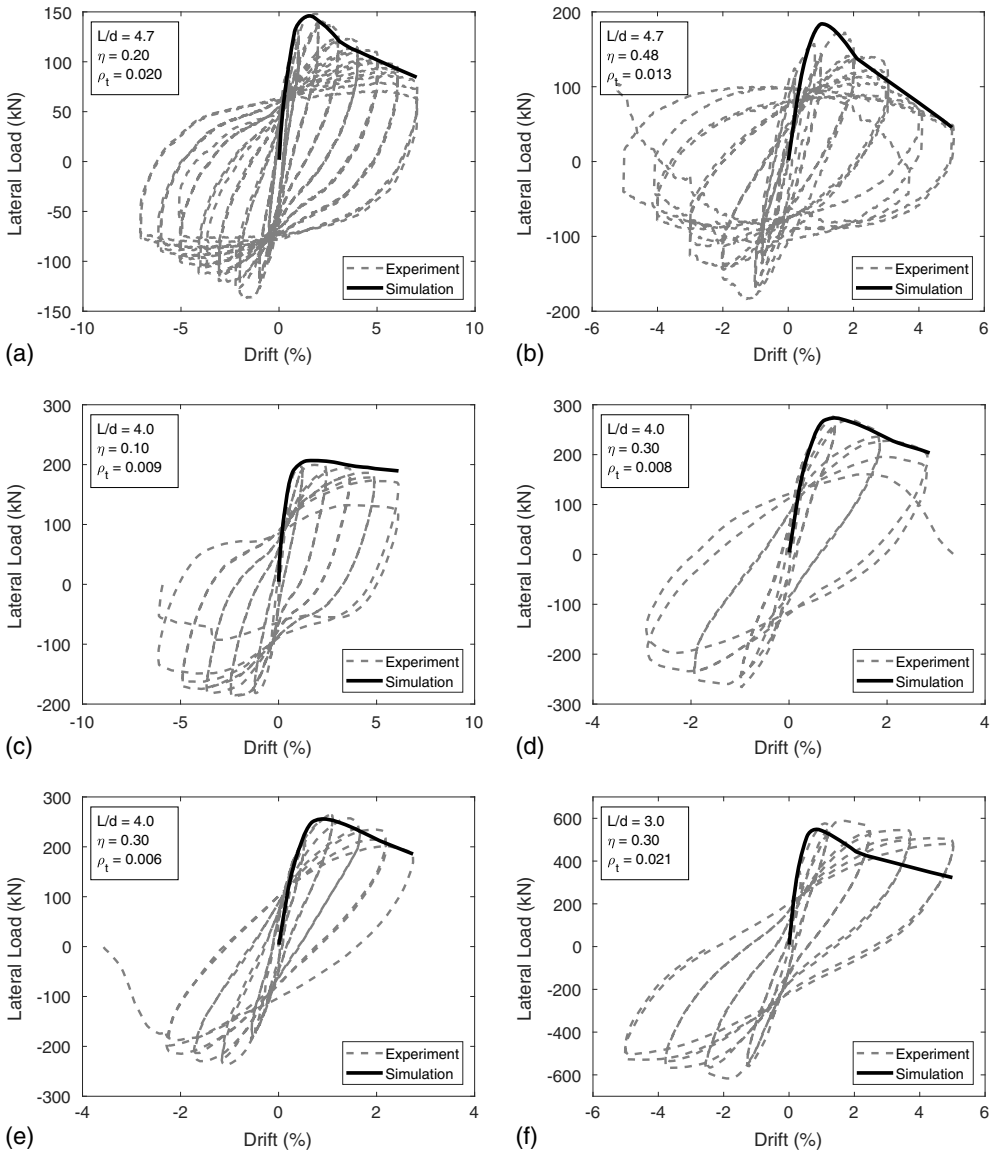

Fig. 10. Predicted and experimentally observed load-displacement response: (a) Saatcioglu and Grira (1999), BG-3; (b) Saatcioglu and Grira (1999), BG-4; (c) Soesianawati et al. (1986), Specimen 1; (d) Soesianawati et al. (1986), Specimen 3; (e) Soesianawati et al. (1986), Specimen 4; and (f) Tanaka and Park (1990), Specimen 7.

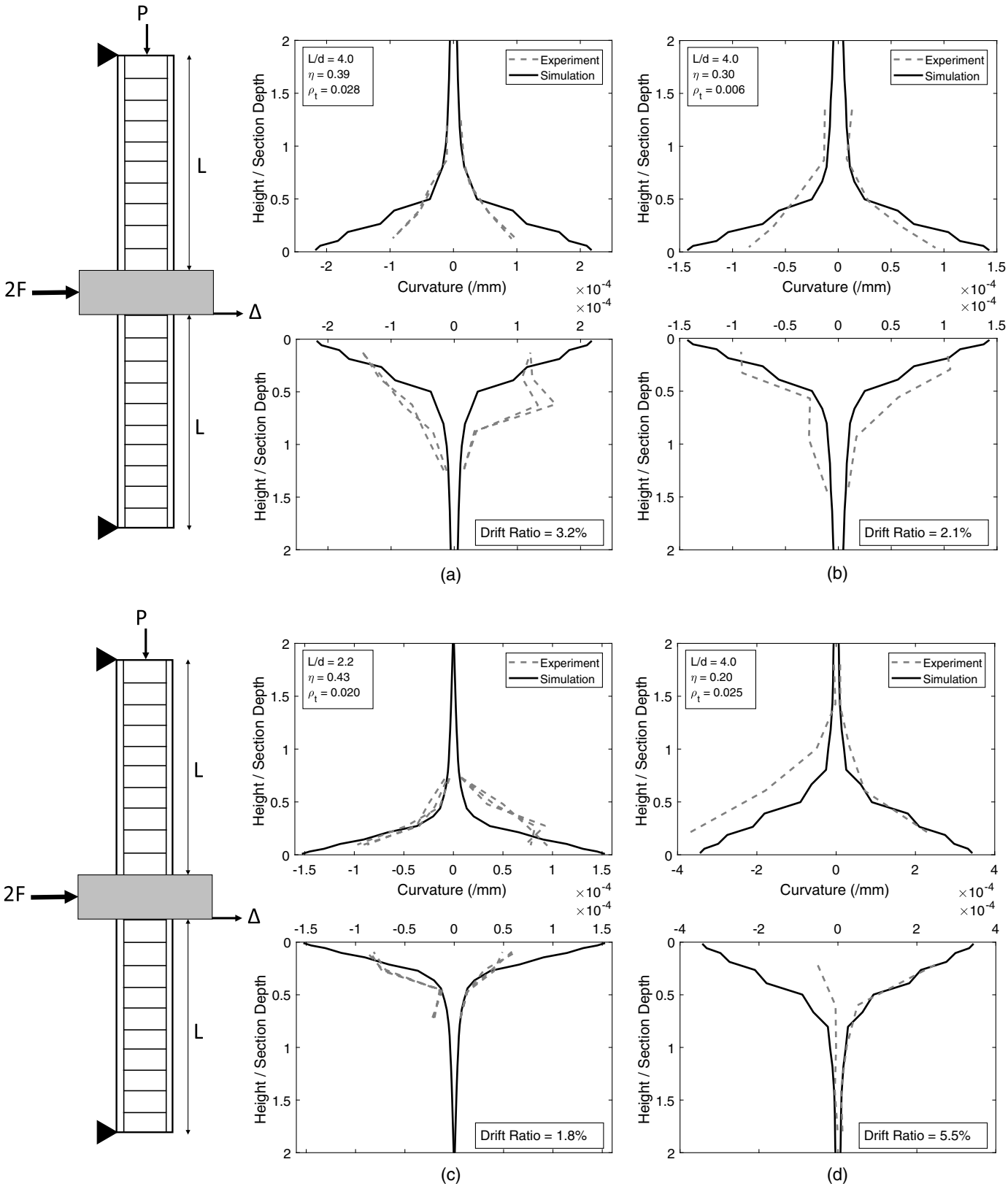

Fig. 11. Predicted and experimentally observed curvature profiles: (a) Ang et al. (1981), Specimen 3; (b) Soesianawati et al. (1986), Specimen 4; (c) Gill et al. (1979), Specimen 3; and (d) Tanaka and Park (1990), Specimen 1.

judged against the monotonic backbone of the experimentally observed responses. It is important to note the distinction between this monotonic backbone (which includes only in-cycle degradation or softening) and the cyclic envelope, which includes both in-cycle and cycle-to-cycle degradation. With this consideration, the following observations are made based on the results in Figs. 9 and 10:

- The load-displacement response predicted by the nonlocal model is in good agreement with the experimental cyclic

data. Reconstructing the backbone envelope from a cyclic test is not straightforward; however, the overall trends of the in-cycle strength degradation are generally well-reproduced.

- In some specimens [e.g., Tanaka and Park (1990), Specimen 7 in Fig. 10(f), and Watson and Park (1989), Specimen 9], the member capacity is underestimated by the simulation. This can be attributed to the uncertainty associated with estimating the confined concrete strength, as reported in the corresponding references (Tanaka and Park 1990; Watson and Park 1989). In general, the discrepancy between the theoretical and experimental confined concrete capacity may be attributed to various factors, including (1) underestiamtion or overestimation of the confined concrete strength and/or strength degradation, and (2) additional confinement effects unaccounted for in the simulation model (for example, the confinement provided by the column base). With these considerations in mind, the results suggest that the selected modified Kent and Park model (Scott et al. 1982) predicts the strength and the softening slope of the confined concrete with reasonable accuracy, despite its simplicity.

Fig. 11 shows the simulated and experimentally measured curvature distributions for four columns at the drift ratios indicated in each figure. These specimens had a double-ended configuration, and therefore the curvature values in the laboratory experiment were recorded along the top and bottom halves. On the other hand, the simulated curvature profile was based on an equivalent cantilever column (Fig. 5) subjected to monotonic displacements; therefore, the same profile was replicated for the top and bottom column halves and for the positive and negative loading directions.

The following factors affected the accuracy of the experimentally measured curvature distribution and must be considered to provide context for the comparison (Fig. 11): (1) the curvature distribution was generally unsymmetric and/or the plastic hinge zone was concentrated in either half of the column, which typically led to large variations in the measured values for the top and bottom halves of the column [e.g., Gill et al. (1979), Specimen 3 and Tanaka and Park (1990), Specimen 1 in Figs. 11(c and d), respectively]; (2) in some specimens [e.g., Ang et al. (1981), Specimen 3 in Fig. 11(a), and Soesianawati et al. (1986), Specimen 3], the maximum curvature was shifted away from the central stub, possibly due to the additional confinement provided by the central stub, which was not accounted for in the simulations; and (3) slightly different curvature measurements at the same drift ratio were recorded for different load cycles [Figs. 11(a and c)] due to cycle-to-cycle degradation of the specimen, which also was not captured in the simulations.

With these considerations in mind, it was concluded that the simulated curvature profile agreed reasonably well with the experimentally measured values, with regard to both the value of the maximum curvature and the length of the plastic hinge zone. The member discretization used to predict the curvature was relatively coarse (10 elements per member, and two Gauss points per element), thus demonstrating the computational efficiency of the proposed approach.

Building upon the preceding discussion of the nonlocal model parameters, the significance of the interaction radius R should be emphasized. A major advantage of the proposed framework is the independence of the value of R with respect to the specimen length, section properties, and mesh size. Instead, this value depends solely on the characteristic length of the softening constitutive relationship, thereby enabling generic and robust simulation of the softening response of RC structural members.

Summary, Conclusions, and Limitations

This study introduced a novel nonlocal formulation framework for the simulation of the postpeak response of RC beam-columns to address the major weaknesses of displacement-based frame elements in the presence of softening constitutive response. The proposed framework consists of a nonlocal DB frame element and a fiber-based nonlocal plasticity model. The framework was implemented in OpenSees, and the performance of the nonlocal model was compared with that of the conventional local model and a large suite of available experimental data. The major findings of this study are summarized as follows:

- The proposed framework successfully eliminates the mesh-dependent strain localization in the presence of concrete softening in compression. The mesh sensitivity study shows that the nonlocal model yields objective global (i.e., load-displacement) and local (i.e., curvature profile) response.
- The proposed framework is able to predict the in-cycle strength degradation (or softening) of RC beam-columns subjected to combined axial loads and monotonically increasing lateral displacements with reasonable accuracy. The numerical examples in this study demonstrate that both the global and local column response are in good agreement with the corresponding experimental test data.
- The nonlocal frame element retains the standard DB finite-element formulation and enriches the formulation with integral terms of existing deformation variables that are straightforward to calculate. The formulation does not incorporate additional boundary conditions or impose stronger continuity requirements on the finite-element interpolation functions. This DB formulation is readily suited for modeling members with distributed loads.
- The nonlocal formulation incorporates a length-scale parameter that is directly informed by the characteristic length associated with the constitutive relationship, and is easily established based

Table 3. Column specimens examined in comparison of confinement models

Column label	Reference	Unconfined concrete strength, f_c (MPa)	Transverse reinforcement ratio, ρ_t	Longitudinal reinforcement ratio, ρ_l
4A5-9	Sheikh and Uzumeri (1980)	40.5	0.024	0.033
B4-20	Sheikh and Uzumeri (1980)	34.7	0.017	0.037
B6-21	Sheikh and Uzumeri (1980)	35.5	0.024	0.037
D4-23	Sheikh and Uzumeri (1980)	35.9	0.017	0.037
D6-24	Sheikh and Uzumeri (1980)	35.9	0.023	0.037
No. 6	Scott et al. (1982)	25.3	0.017	0.019
No. 2	Scott et al. (1982)	25.3	0.018	0.018
A	Razvi (1988)	32.0	0.013	0.031
B	Razvi (1988)	29.0	0.027	0.031
A	Razvi (1988)	39.0	0.028	0.016

on the uniaxial stress-strain relationship determined by the concrete confinement model. This value does not depend on the member length or section geometry, and is not based on an empirical plastic hinge relationship.

- The nonlocality in the proposed formulation is enforced at the constitutive level through an appropriately enriched nonlocal plasticity model. This aspect lends the length-scale parameter the straightforward interpretation adopted in this study. However, it also means that the model requires transfer of the deformation data between different integration points (typically over multiple elements) to calculate spatial averages of the deformation variables.

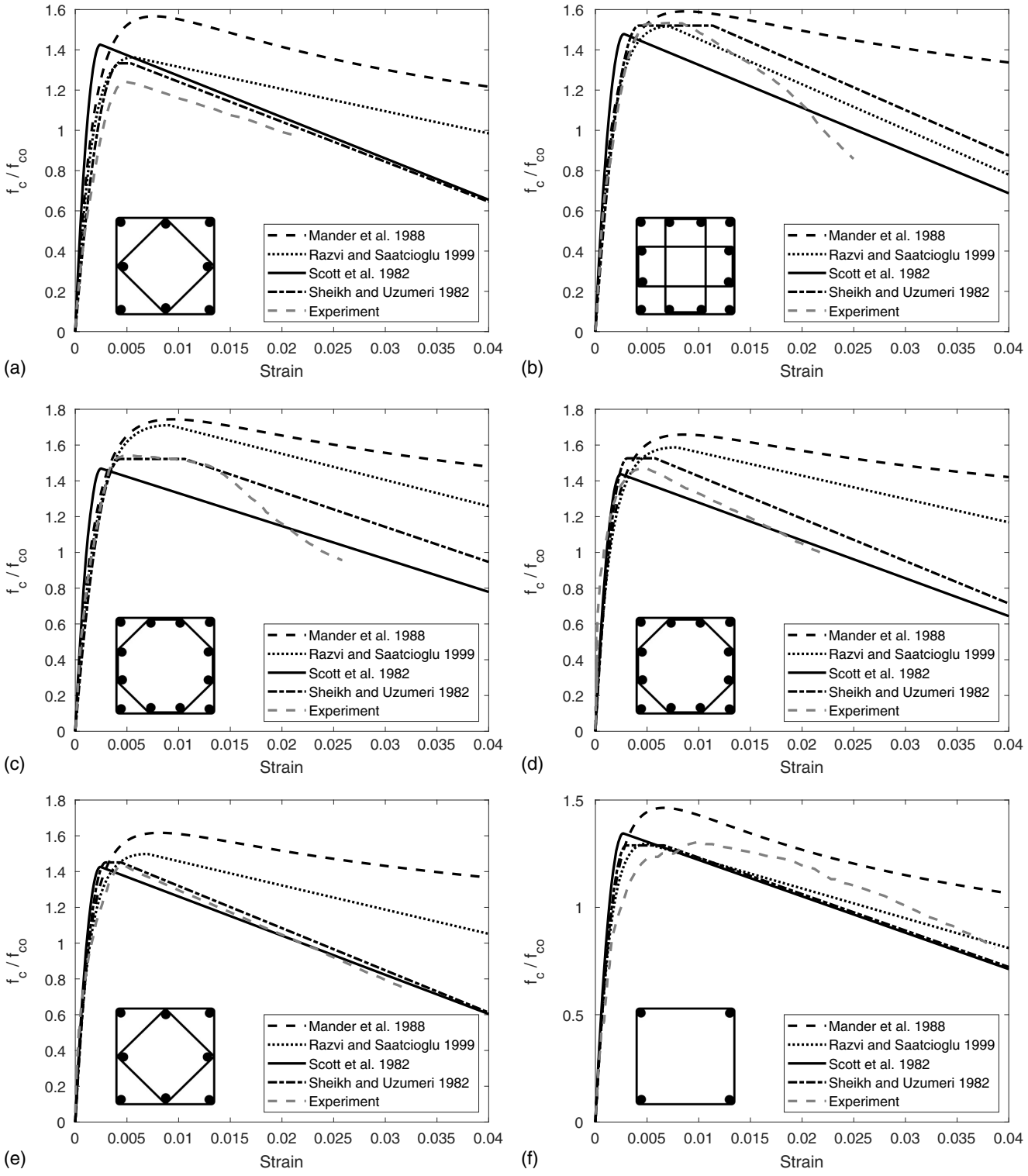

Fig. 12. Observed and predicted uniaxial response of RC columns by different confinement models: (a) Sheikh and Uzumeri (1980), 4A5-9; (b) Sheikh and Uzumeri (1980), 4B4-20; (c) Sheikh and Uzumeri (1980), 4D4-23; (d) Scott et al. (1982), Specimen 2; (e) Scott et al. (1982), Specimen 6; and (f) Razvi (1988), 16B.

- Because of the aforementioned property, the proposed nonlocal fiber-based frame model is computationally more expensive than lumped plasticity models. However, the efficacy of fiber-based models (enabling the spread of plasticity and capturing P-M interaction) is the main motivation for the formulation developed in this study. A quantitative comparison of the integral nonlocal formulation presented in this study against recent gradient-based frame element formulations in the literature may be needed to assess the performance and computational expense associated with each.

The nonlocal constitutive relation employed in this study is suited for monotonic loading only, and it represents a rather simplified approximation of the nonlinear concrete response. Additionally, the proposed framework focused on the simulation of concrete softening in compression, and neglected other localized phenomena at the cross-section level (e.g., rebar buckling). Therefore, future work will focus on (1) developing a more realistic nonlocal uniaxial constitutive model for concrete which incorporates both strength and stiffness degradation and is suited for cyclic and seismic loading applications, and (2) incorporating the effects of damage of other components of the RC cross-section, namely buckling of the steel rebar in compression and fracture in tension; these phenomena can be incorporated in the fiber-based frame model by using uniaxial material models for steel bars with nonlocal softening, as in the model presented by Kolwankar et al. (2017).

Appendix. Selection of Confined Concrete Model

In frame-element models utilizing a fiber section discretization, the effect of the confining transverse reinforcement in the column is conventionally modeled in an indirect manner by enhancing the strength and postpeak response of the confined concrete. Several models in the literature provide frameworks for estimating the confined concrete properties; examples include Mander et al. (1988), the modified Kent and Park model (Scott et al. 1982), Sheikh and Uzumeri (1982), Razvi and Saatcioglu (1999), and Hoshikuma et al. (1997). In the present numerical investigation, accurate prediction of the confined concrete strength and strength degradation was essential for consistency of the comparison of the simulation models and experimental test data. Therefore, it was deemed necessary to investigate different confinement models to determine a suitable model for estimating the confined concrete properties.

The experimental stress-strain curves of 10 column specimens tested under pure axial load in three different studies (Scott et al. 1982; Sheikh and Uzumeri 1980; Razvi 1988) were used to assess the performance of four confinement models. The properties of the column specimens are presented in Table 3; these specimens were selected to span a range of transverse reinforcement ratios and tie configurations. For each column, the uniaxial stress strain curves predicted by the confinement models [Mander et al. (1988); the modified Kent and Park model by Scott et al. (1982); Sheikh and Uzumeri (1982); and Razvi and Saatcioglu (1999)] were compared with the corresponding experimental stress-strain curve. The main material parameters considered in the comparison were the confined concrete maximum stress f_{cc} and the softening slope E_{dc}.

Fig. 12 shows representative results of the comparison in which the predictions of the four confinement models are laid atop the experimentally observed response. Model predictions usually produce best fits to the test data to which the model was calibrated; therefore, the main objective of the comparison was to select a model which consistently produced reasonable predictions across different data sets. The results suggest that the Mander et al. (1988) model generally underestimates the strength degradation of the confined concrete, and in some cases, overestimates the strength. For the selected specimens, the comparison indicates that the Razvi and Saatcioglu (1999), modified Kent and Park (Scott et al. 1982), and Sheikh and Uzumeri (1982) models tend to provide relatively reasonable estimates of the strength and degradation rate, with the Razvi and Saatcioglu model occasionally overestimating the capacity. The modified Kent and Park model was selected for the present study because it (1) provides reasonably accurate estimates of the confined concrete parameters, and (2) produces a relatively simple stress-strain curve that can be conveniently approximated with the bilinear material model adopted in the present study (Fig. 13).

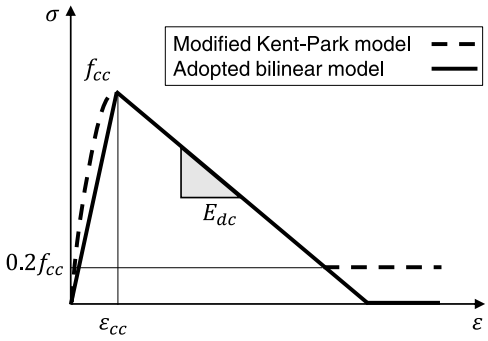

Fig. 13. Adopted material model for confined concrete.

Acknowledgments

This work was supported by the National Science Foundation (Grant No. CMMI 1434300) and graduate assistantships from the University of California at Davis. The findings and opinions presented in this paper are entirely those of the authors.

References

Addessi, D., and V. Ciampi. 2007. "A regularized force-based beam element with a damage-plastic section constitutive law." *Int. J. Numer. Methods Eng.* 70 (5): 610–629. https://doi.org/10.1002/nme.1911.

Ang, B. G., M. J. N. Priestley, and R. Park. 1981. "Ductility of reinforced concrete bridge piers under seismic loading." Ph.D. thesis, Dept. of Civil Engineering, Univ. of Canterbury.

Atalay, M. B., and J. Penzien. 1975. *The seismic behavior of critical regions of reinforced concrete components as influenced by moment, shear and axial force*. Technical Rep. Berkeley, CA: Univ. of California.

Bazant, Z. P. 1976. "Instability, ductility, and size effect in strain-softening concrete." *J. Eng. Mech. Div.* 102 (2): 331–344.

Bazant, Z. P. 1982. "Crack band model for fracture of geomaterials." In *Proc., 4th Int. Conf. of Numerical Methods in Geomechanics*. Edmonton, AB, Canada: Citeseer.

Bažant, Z. P., and T. B. Belytschko. 1985. "Wave propagation in a strain-softening bar: Exact solution." *J. Eng. Mech.* 111 (3): 381–389. https://doi.org/10.1061/(ASCE)0733-9399(1985)111:3(381).

Bažant, Z. P., and G. Di Luzio. 2004. "Nonlocal microplane model with strain-softening yield limits." *Int. J. Solids Struct.* 41 (24): 7209–7240.

Bažant, Z. P., and M. Jirásek. 2002. "Nonlocal integral formulations of plasticity and damage: Survey of progress." *J. Eng. Mech.* 128 (11): 1119–1149. https://doi.org/10.1061/(ASCE)0733-9399(2002)128:11(1119).

Bažant, Z. P., and F.-B. Lin. 1988a. "Non-local yield limit degradation." *Int. J. Numer. Methods Eng.* 26 (8): 1805–1823. https://doi.org/10.1002/nme.1620260809.

Bažant, Z. P., and F.-B. Lin. 1988b. "Nonlocal smeared cracking model for concrete fracture." *J. Struct. Eng.* 114 (11): 2493–2510. https://doi.org/10.1061/(ASCE)0733-9445(1988)114:11(2493).

Bažant, Z. P., and B. H. Oh. 1983. "Crack band theory for fracture of concrete." *Matériaux et Constr.* 16 (3): 155–177. https://doi.org/10.1007/BF02486267.

Bažant, Z. P., J. Pan, and G. Pijaudier-Cabot. 1987. "Softening in reinforced concrete beams and frames." *J. Struct. Eng.* 113 (12): 2333–2347. https://doi.org/10.1061/(ASCE)0733-9445(1987)113:12(2333).

Bažant, Z. P., and G. Pijaudier-Cabot. 1989. "Measurement of characteristic length of nonlocal continuum." *J. Eng. Mech.* 115 (4): 755–767. https://doi.org/10.1061/(ASCE)0733-9399(1989)115:4(755).

Berry, M., M. Parrish, and M. Eberhard. 2004. *PEER structural performance database user's manual (version 1.0)*. Berkeley, CA: Univ. of California.

Brinkgreve, R. B. J. 1994. "Geomaterial models and numerical analysis of softening." Ph.D. thesis, Delft Univ. of Technology.

Clough, R. W., K. L. Benuska, and E. L. Wilson. 1965. "Inelastic earthquake response of tall buildings." In Vol. 11 of *Proc., 3rd World Conf. on Earthquake Engineering*. New Zealand.

Coleman, J., and E. Spacone. 2001. "Localization issues in force-based frame elements." *J. Struct. Eng.* 127 (11): 1257–1265. https://doi.org/10.1061/(ASCE)0733-9445(2001)127:11(1257).

El-Tawil, S., and G. G. Deierlein. 1998. "Stress-resultant plasticity for frame structures." *J. Eng. Mech.* 124 (12): 1360–1370. https://doi.org/10.1061/(ASCE)0733-9399(1998)124:12(1360).

Feng, D., X. Ren, and J. Li. 2015. "Implicit gradient delocalization method for force-based frame element." *J. Struct. Eng.* 142 (2): 04015122. https://doi.org/10.1061/(ASCE)ST.1943-541X.0001397.

Filippou, F., and A. Saritas. 2006. "A beam finite element for shear-critical RC beams." *ACI Special Publ.* 237: 295–310.

Giberson, M. F. 1967. "The response of nonlinear multi-story structures subjected to earthquake excitation." Ph.D. thesis, Dept. of Engineering and Applied Science, California Institute of Technology.

Gill, W. D., R. Park, and M. J. N. Priestley. 1979. "Ductility of rectangular reinforced concrete columns with axial load." M.S. thesis, Dept. of Civil Engineering, Univ. of Canterbury.

Grassl, P., and M. Jirásek. 2006. "Damage-plastic model for concrete failure." *Int. J. Solids Struct.* 43 (22): 7166–7196. https://doi.org/10.1016/j.ijsolstr.2006.06.032.

Hoshikuma, J., K. Kawashima, K. Nagaya, and A. W. Taylor. 1997. "Stress-strain model for confined reinforced concrete in bridge piers." *J. Struct. Eng.* 123 (5): 624–633. https://doi.org/10.1061/(ASCE)0733-9445(1997)123:5(624).

Hughes, T. J., J. A. Cottrell, and Y. Bazilevs. 2005. "Isogeometric analysis: CAD, finite elements, NURBS, exact geometry and mesh refinement." *Comput. Methods Appl. Mech. Eng.* 194 (39–41): 4135–4195. https://doi.org/10.1016/j.cma.2004.10.008.

Jansen, D. C., and S. P. Shah. 1997. "Effect of length on compressive strain softening of concrete." *J. Eng. Mech.* 123 (1): 25–35. https://doi.org/10.1061/(ASCE)0733-9399(1997)123:1(25).

Jirásek, M., and S. Rolshoven. 2003. "Comparison of integral-type nonlocal plasticity models for strain-softening materials." *Int. J. Eng. Sci.* 41 (13–14): 1553–1602. https://doi.org/10.1016/S0020-7225(03)00027-2.

Jirásek, M., and T. Zimmermann. 1998. "Rotating crack model with transition to scalar damage." *J. Eng. Mech.* 124 (3): 277–284. https://doi.org/10.1061/(ASCE)0733-9399(1998)124:3(277).

Kanda, M., N. Shirai, H. Adachi, and T. Sato. 1988. "Analytical study on elasto-plastic hysteretic behaviors of reinforced concrete members." *Trans. Jpn. Concr. Inst.* 10 (1): 257–264.

Kolwankar, S., A. Kanvinde, M. Kenawy, and S. Kunnath. 2017. "Uniaxial nonlocal formulation for geometric nonlinearity-induced necking and buckling localization in a steel bar." *J. Struct. Eng.* 143 (9): 04017091. https://doi.org/10.1061/(ASCE)ST.1943-541X.0001827.

Kono, S., and F. Watanabe. 2000. "Damage evaluation of reinforced concrete columns under multiaxial cyclic loadings." In *Proc., 2nd US-Japan Workshop on Performance-Based Earthquake Engineering Methodology for Reinforced Concrete Building Structures*, 221–231. Berkeley, CA: Pacific Earthquake Engineering Research Center.

Mander, J. B., M. J. N. Priestley, and R. Park. 1988. "Observed stress-strain behavior of confined concrete." *J. Struct. Eng.* 114 (8): 1827–1849. https://doi.org/10.1061/(ASCE)0733-9445(1988)114:8(1827).

McKenna, F., G. L. Fenves, and M. H. Scott. 2000. "Open system for earthquake engineering simulation." Univ. of California. http://opensees.berkeley.edu.

Menegotto, M., and P. Pinto. 1973. "Method of analysis for cyclically loaded reinforced concrete plane frames including changes in geometry and inelastic behavior of elements under combined normal force and bending." In *Proc., IABSE Symp. on Resistance and Ultimate Deformability of Structures Acted on by Well Defined Repeated Loads, Final Report*. Zurich, Switzerland: International Association for Bridge and Structural Engineering.

Peerlings, R., M. Geers, R. De Borst, and W. Brekelmans. 2001. "A critical comparison of nonlocal and gradient-enhanced softening continua." *Int. J. Solids Struct.* 38 (44–45): 7723–7746. https://doi.org/10.1016/S0020-7683(01)00087-7.

Pijaudier-Cabot, G., and Z. P. Bažant. 1987. "Nonlocal damage theory." *J. Eng. Mech.* 113 (10): 1512–1533. https://doi.org/10.1061/(ASCE)0733-9399(1987)113:10(1512).

Planas, J., M. Elices, and G. V. Guinea. 1993. "Cohesive cracks versus nonlocal models: Closing the gap." *Int. J. Fract.* 63 (2): 173–187. https://doi.org/10.1007/BF00017284.

Powell, G. H., and P. F.-S. Chen. 1986. "3D beam-column element with generalized plastic hinges." *J. Eng. Mech.* 112 (7): 627–641. https://doi.org/10.1061/(ASCE)0733-9399(1986)112:7(627).

Pugh, J. S., L. N. Lowes, and D. E. Lehman. 2015. "Nonlinear line-element modeling of flexural reinforced concrete walls." *Eng. Struct.* 104: 174–192. https://doi.org/10.1016/j.engstruct.2015.08.037.

Razvi, S., and M. Saatcioglu. 1999. "Confinement model for high-strength concrete." *J. Struct. Eng.* 125 (3): 281–289. https://doi.org/10.1061/(ASCE)0733-9445(1999)125:3(281).

Razvi, S. R. 1988. "Behavior of reinforced concrete columns confined with welded wire fabric." M.A.Sc. thesis, Dept. of Civil Engineering, Univ. of Ottawa.

Rolshoven, S. 2003. "Nonlocal plasticity models for localized failure." Ph.D. thesis, Civil Engineering Section, École Polytechnique Fédérale de Lausanne.

Saatcioglu, M., and M. Grira. 1999. "Confinement of reinforced concrete columns with welded reinforced grids." *ACI Struct. J.* 96 (1): 29–39.

Scott, B. D., R. Park, and M. J. N. Priestley. 1982. "Stress-strain behavior of concrete confined by overlapping hoops at low and high strain rates." *ACI J.* 79 (1): 13–27.

Scott, M. H., and G. L. Fenves. 2006. "Plastic hinge integration methods for force-based beam-column elements." *J. Struct. Eng.* 132 (2): 244–252. https://doi.org/10.1061/(ASCE)0733-9445(2006)132:2(244).

Sheikh, S. A., and S. M. Uzumeri. 1980. "Strength and ductility of tied concrete columns." *J. Struct. Div.* 106 (5): 1079–1102.

Sheikh, S. A., and S. M. Uzumeri. 1982. "Analytical model for concrete confinement in tied columns." *J. Struct. Div.* 108 (12): 2703–2722.

Sideris, P., and M. Salehi. 2016. "A gradient inelastic flexibility-based frame element formulation." *J. Eng. Mech.* 142 (7): 04016039. https://doi.org/10.1061/(ASCE)EM.1943-7889.0001083.

Soesianawati, M. T., R. Park, and M. J. N. Priestley. 1986. "Limited ductility design of reinforced concrete columns." Ph.D. thesis, Dept. of Civil Engineering, Univ. of Canterbury.

Spacone, E., F. C. Filippou, and F. F. Taucer. 1996a. "Fibre beam-column model for non-linear analysis of R/C frames. Part I: Formulation." *Earthquake Eng. Struct. Dyn.* 25 (7): 711–725. https://doi.org/10.1002/(SICI)1096-9845(199607)25:7<711::AID-EQE576>3.0.CO;2-9.

Spacone, E., F. C. Filippou, and F. F. Taucer. 1996b. "Fibre beam-column model for non-linear analysis of R/C frames. Part II: Applications." *Earthquake Eng. Struct. Dyn.* 25 (7): 727–742. https://doi.org/10.1002/(SICI)1096-9845(199607)25:7<727::AID-EQE577>3.0.CO;2-O.

Strömberg, L., and M. Ristinmaa. 1996. "FE-formulation of a nonlocal plasticity theory." *Comput. Methods Appl. Mech. Eng.* 136 (1–2): 127–144. https://doi.org/10.1016/0045-7825(96)00997-8.

Tanaka, H., and R. Park. 1990. "Effect of lateral confining reinforcement on the ductile behaviour of reinforced concrete columns." Ph.D. thesis, Dept. of Civil Engineering, Univ. of Canterbury.

Valipour, H. R., and S. J. Foster. 2009. "Nonlocal damage formulation for a flexibility-based frame element." *J. Struct. Eng.* 135 (10): 1213–1221. https://doi.org/10.1061/(ASCE)ST.1943-541X.0000054.

Van Mier, J. G. M. 1984. "Strain-softening of concrete under multiaxial loading conditions." Ph.D. thesis, Eindhoven Univ. of Technology.

Van Mier, J. G. M., S. P. Shah, M. Arnaud, J. P. Balayssac, A. Bascoul, S. Choi, D. Dasenbrock, G. Ferrara, C. French, and M. E. Gobbi. 1997. "Strain-softening of concrete in uniaxial compression." *Mater. Struct.* 30 (4): 195–209. https://doi.org/10.1007/BF02486177.

Vonk, R. A. 1993. *A micromechanical investigation of solftening of concrete loaded in compression*. Technical Rep. Eindhoven, Netherlands: Eindhoven Univ. of Technology.

Watson, S., and R. Park. 1989. "Design of reinforced concrete frames of limited ductility." Ph.D. thesis, Dept. of Civil Engineering, Univ. of Canterbury.

Zahn, F. A., R. Park, and M. J. N. Priestley. 1985. "Design of reinforced concrete bridge columns for strength and ductility." Ph.D. thesis, Dept. of Civil Engineering, Univ. of Canterbury.

Zhang, G., and K. Khandelwal. 2016. "Modeling of nonlocal damage-plasticity in beams using isogeometric analysis." *Comput. Struct.* 165: 76–95. https://doi.org/10.1016/j.compstruc.2015.12.006.

Zienkiewicz, O. C., and R. L. Taylor. 2005. *The finite element method for solid and structural mechanics*. Oxford, UK: Butterworth-Heinemann.